Journal of Membrane Science, 78 (1993) 197–216
Elsevier Science Publishers B.V., Amsterdam

Microporous hollow fibre membrane modules as gas–liquid contactors. Part 1. Physical mass transfer processes

A specific application: Mass transfer in highly viscous liquids

H. Kreulen*, C.A. Smolders, G.F. Versteeg** and W.P.M. van Swaaij
Faculty of Chemical Technology, University of Twente, P.O. Box 217, 7500 AE Enschede (The Netherlands)

(Received March 26, 1992; accepted in revised form November 20, 1992)

Abstract

Gas–liquid mass transfer has been studied in a membrane module with non-wetted microporous fibres in the laminar flow regime. This new type of gas/liquid contactor can be operated stabily over a large range of gas and liquid flows because gas and liquid phase do not influence each other directly. Therefore foam is not formed in the module, gas bubbles are not entrained in the liquid flowing out of the reactor and the separation of both phases can be achieved very easily. These phenomena often limit the applicability of conventional contactors, e.g. a bubble column which was also studied in the present work. The large mass transfer area of a bundle of small fibres offers the possibility of creating a compact gas/liquid mass exchanger. However, owing to the small channels in and around the fibres the flow of either gas or liquid becomes laminar which reduces the mass transfer capacity of the module. Therefore the mass transfer coefficients in the laminar flow regime were determined experimentally. For mass transfer determined by the transport in the liquid phase it was found that the active mass transfer area is equal to the total membrane area, regardless the porosity of the fibre. For processes with liquid flowing through the fibres, the influence of fibre diameter, diffusivity in the liquid, liquid viscosity and liquid velocity on mass transfer can be correlated extremely well with the Graetz–Lévèque solution derived for the analogous case of heat transfer. For liquid flowing around regularly packed fibres mass transfer was described satisfactory with a correlation derived from a numerical solution for the similar heat transfer problem [Miyatake and Iwashita, Int. J. Heat Mass Transf., 33 (1990) 416]. Correlating mass transfer in liquid flowing around irregularly packed fibres was not possible because of the undefined dimensions of the different channels between the fibres.

Keywords: mass transfer; microporous membranes; absorption

---

*Present address: AKZO Chemicals, P.O. Box 10, 7400 AA Deventer, The Netherlands.
**To whom correspondence should be addressed.

1. Introduction

A microporous membrane can be used to create a fixed interfacial area between gas and liquid phase in gas/liquid processes. Depending on the interaction of the membrane material, the liquid and the pressures on each side of the membrane, either wetted or non-wetted membrane conditions may be realised. In literature the membrane material is often referred to as hydrophilic or hydrophobic. In this paper the only important issue is the medium which is present in the pores of the membrane, gas or liquid. Therefore the distinction between wetted and non-wetted is made in stead of hydrophilic versus hydrophobic. In a wetted membrane the pores are filled with liquid and thus a stagnant liquid layer is present between the free gas and liquid phase. A stagnant layer of gas is present in the pores of a non-wetted membrane.

Kreulen et al. [1] carried out mass transfer experiments with flat horizontal membranes in a stirred cell reactor. It was found that the mass transfer resistance of non-wetted membranes is relatively small compared to the resistances in gas and liquid phase. In wetted membranes however, the mass transfer resistance of the liquid layer is much larger. In these membrane systems mass transfer resistance is mainly determined by the membrane. From this result it was concluded that non-wetted membranes are to be preferred for the creation of a fixed interface in gas/liquid absorbers with membranes.

The absorption rate that can be obtained in a contactor is the product of the interfacial area and the mass transfer coefficients. It will be demonstrated that in conventional contactors the mass transfer coefficients are higher than those in hollow fibre membrane modules. This can be attributed to two effects. (1) For the system with a membrane at the interface the mass transfer process is determined by three mass transfer resistances in series: resistance in the gas, in the stagnant layer of the membrane and in the liquid. For systems with a free uncovered gas/liquid interface the stagnant film is not present and therefore only the two mass transfer resistances in the gas and the liquid have to be considered. In the free gas and liquid phase the mass transfer resistance is determined by diffusion and convection while in the membrane the mass transfer resistance only depends on diffusion. (2) The hydrodynamic state of the gas and liquid flow must be considered. Mass transfer resistances are smaller in the turbulent than in the laminar regime. In the hollow fibre membrane contactor the flow is usually laminar because of the small fibre diameters and the small distance between the fibers.

The contact area between gas and liquid of the hollow fibre membrane contactor can be substantially larger than in conventional gas/liquid contacting equipment. For instance, the specific exchange area with a fibre of 1×10^{-3} m diameter can be about 3000 m^2/m^3 while in bubble columns, sieve trays or packed beds this area is around 800 m^2/m^3 at a maximum (Laurent and Charpentier [2], Van Landeghem [3]). For hollow fibre modules numbers of 8,000 m^2/m^3 are reported by Matson et al. [4].

It can be concluded that although the mass transfer coefficients in hollow fibre modules are smaller than in conventional contactors, the substantial increase of the interfacial area can result in a more efficient absorber.

For the selection of a gas/liquid contactor the absorption rate is not the only property which must be taken into account. Another distinct feature of the hollow fibre module is that flow of gas and liquid do not influence each other. This results in a larger operation flexibility than in the reactors mentioned above, which are re-

stricted severely by phenomena like flooding, loading etc. However, it must be noted that due to the small fibres and the close packing of the fibres a relatively large pressure drop over the liquid phase is obtained.

Another selection criterion for contactors is the separation of gas and liquid flow which can be of particular interest when gases are ab- or desorbed in or from viscous liquids. Generally, small stagnant bubbles are formed which leave the absorber with the liquid phase. Next, in the separator care must be taken not to desorb the gas again while these bubbles are removed. In the hollow fibre modules gas and liquid flow are never mixed so the separator stage can be omitted.

In the present study the application of the hollow fibre membranes as fixed gas/liquid interface is investigated. Experiments with hollow fibre modules were carried out in which fibre diameter, fibre length, diffusion coefficient and liquid flow velocities were varied. The results of these experiments are translated to dimensionless mass transfer correlations which can be used in scaling up of the process.

The measured mass transfer rates are compared with mass transfer rates measured in a small bubble column. On the basis of these experimental results a comparison is made between the absorption capacity of the hollow fibre membrane and the bubble column. Special attention has been paid to mass transfer processes in highly viscous liquids to see whether absorption without stagnant bubble formation is possible in the hollow fibre membrane module.

2. Theory

Physical absorption from a gas through a porous (gas filled) membrane in a liquid exists of three steps. Firstly, the transfer from the gas to the membrane wall, next the transfer through the stagnant gas in the pores of the membrane

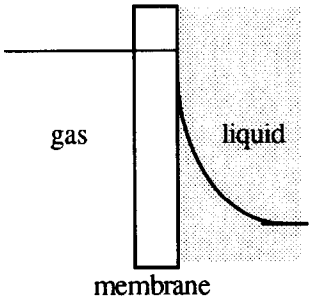

Fig. 1. Concentration profile for mass transfer in a gas/membrane/liquid system, with a pure gas an a non-wetted membrane.

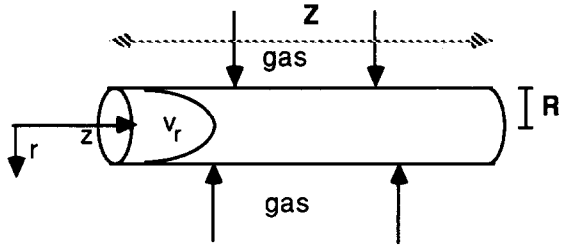

Fig. 2. Coordinate system in a hollow fibre membrane.

and last, the transfer from the membrane/liquid interface into the bulk of the liquid.

In this study the absorption of a pure gas into a liquid flowing through the lumen of the fibres is reported. Therefore the mass transfer resistance in the gas phase does not have to be considered. The membrane permeability should be large enough to supply gas at the interface. This situation is schematically presented in Fig. 1.

The concentration profiles in the liquid can be calculated from the differential mass balance (eqn. 1) that describes diffusion and forced convection in a medium that flows laminarly through a circular pipe (Fig. 2). Axial diffusion is neglected because the concentration gradient in axial direction will be much smaller than the concentration gradient in radial direction.

$$v_r \frac{\partial C}{\partial z} = D\left[\frac{1}{r}\frac{\partial}{\partial r}\left(r\frac{\partial C}{\partial r}\right)\right] \quad (1)$$

With boundary conditions:

$$C_{r=R}=C_w=mC_g, \quad 0\leqslant z\leqslant Z$$

$$\left(\frac{\partial C}{\partial r}\right)_{r=0}=0, \quad 0\leqslant z\leqslant Z$$

For a fully developed laminar flow in a tube the velocity profile can be described by:

$$v_r=2v_m\left[1-\left(\frac{r}{R}\right)^2\right] \tag{2}$$

The analogous differential equation for the heat transfer problem in laminar flow through a circular duct was solved by Graetz [5,6], extended by Lévèque [7] and is discussed in extenso by Jakob [8]. From the calculated concentration profiles, fluxes and mass transfer coefficients can be deduced. The mass transfer coefficient is calculated according to eqn. (3), in which C_z is the mixing cup concentration in the liquid at the axial coordinate z.

$$k_L=\frac{J}{C_w-C_z} \tag{3}$$

Two asymptotic correlations are valid for the dimensionless mass transfer coefficients.

$$Sh=1.62\left(Re\,Sc\frac{d}{Z}\right)^{1/3}=1.62\left(\frac{vd^2}{DZ}\right)^{1/3}=1.62Gz^{1/3} \tag{4a}$$

$$Sh=3.67 \tag{4b}$$

Equation (4a) is valid for the entrance region where the concentration profile has to build up, $Re\,Sc\,d/Z>20$. Equation (4b) must be applied for long tubes where the concentration profile is completely developed, which means that the profile has a constant shape over the radius, $Re\,Sc\,d/Z<10$. ($Re\,Sc\,d/Z$) is the Graetz number. Some authors also define this number as $Q_v/(DZ)$, which differs a factor of $\pi/4$ from the definition in this study.

3. Literature

A limited amount of papers concerning the experimental verification of eqn. (4) is available. For heat transfer applications Sieder and Tate [9] developed an expression similar to eqn. (4a) for the Nusselt number form their experimental results. In their empirically obtained correlation, they also incorporated the influence of temperature on viscosity.

To study mass transfer the dissolution of pipes made of soluble solid material was studied by a few authors. Linton and Sherwood [10] used pipes constructed of benzoic and cinnamic acid which dissolved in water. From the weight loss of the pipes the mass transfer coefficients were calculated. Their results are in close agreement with eqn. (4a).

Goldman and Barrett [11] studied the dissolution of sodium chloride in water/glycerol mixtures. The measured weight loss was in accordance with the weight loss predicted by their theoretical solution, which is similar to the one derived by Lévèque but also the influence of the solute on viscosity and density is taken into account. Therefore, the diffusion process is influenced by the solute. This approach of the dissolution process is necessary when a very soluble material is used, which was the case in the experiments of Goldman and Barret.

Kafes and Clump [12] studied mass transfer with tubular dialysis membranes. On the outside of the membrane a saturated salt solution was present while the inside of the membrane was flown through with city water. Mass transfer coefficients for the laminar flow through the tube side were calculated from overall measured fluxes. They could not be correlated with eqn. (4a). This might be due to convective flow through the membrane resulting in higher mass transfer coefficients.

Recently, non-wetted microporous fibres were used to study mass transfer in pipe flow. In contrast to the studies with dialysis mem-

branes water is not absorbed in the fibre wall. Therefore mass transfer in the free liquid can be measured directly. Yang and Cussler [13] studied gas–liquid mass transfer. They determined the influence of velocity on the mass transfer coefficient for laminar flow empirically by desorbing O_2 from water. The results of experiments with liquid flowing through the fibres corresponded to eqn. (4a).

Qi and Cussler [14] measured mass transfer coefficients with the absorption of CO_2 in a solution of sodium hydroxide. It might be expected that the mass transfer process was influenced by the chemical reaction between hydroxide and carbon dioxide (Kreulen [15]). However, the dependency of the overall mass transfer coefficient on the liquid velocity was found to be in accordance with eqn. (4a).

When the porous fibres are used in absorption experiments the question arises which area of the porous membrane should be taken as the exchanging area. Either the open pore area can be chosen or the area of the total membrane (i.e. pores+polymer). In heat transfer and mass transfer with soluble walls, the complete tube area is taking part in the transfer process. This assumption is also used in the solution of eqn. (1).

Wakeham and Mason [16] developed a general mathematical model to describe diffusion through perforated layers into a stagnant boundary layer. One of their asymptotic solutions may be applicable to the absorption process with porous membranes. The main parameters which must be considered are the distance between two pores and the thickness of the boundary layer. In the present work these parameters will be evaluated for two types of membranes with different porosities to determine which area should be taken.

The mass balance for absorption in the liquid flowing around the fibres cannot be solved as easily as with liquid through the fibres which is in fact a two dimensional problem. The interaction of the different fibres must be taken into account and therefore a three dimensional problem is obtained. A simple two dimensional approximation of the fibre bundle is flow through an annulus.

Lin et al. [17] used an electrochemical method for the determination of mass transfer coefficients in such a geometry. This method cannot be used in real pipe flow because it needs the use of two electrodes (Mizushina [18]). One being the tube wall while the other electrode must be placed in the liquid stream, which disturbs the flow. Lin et al. translated their experimental results with the use of the hydraulic diameter to give results which corresponded to eqns. (4).

Yang and Cussler [13] also carried out absorption experiments with liquid flow around the fibres. Like Lin et al. they also used the hydraulic diameter for the translation of their experimental results to the dimensionless correlations. The mass transfer coefficients were found to depend almost linearly on the liquid velocity. This is not in agreement with eqns. (4).

Recently, a numerical solution was presented for heat transfer in the shell side of a shell-tube heat exchanger by Miyatake and Iwashita [19]. From their numerical results dimensionless Nusselt correlations were derived which can also be useful in the interpretation of experimental mass transfer data for hollow fibre modules (Appendix A). However, there is one very important difference between this type of heat exchanger and a commercially available membrane module. The tubes are welded in a regular packing while the fibres are not positioned regularly during the construction of the modules. In the present work a module with regularly spaced fibres was used to compare its performance with that of modules with irregularly spaced fibres.

Due to differences in fibre diameter or in the channel widths between the fibres, substantial

maldistribution of the liquid around the fibres can occur. This can have a large influence on the efficiency of mass transfer as is shown in the next section.

4. Effects of maldistribution of phases in hollow fibre modules

In a lot of mass exchanging equipment a non-ideal distribution of gas and liquid phase caused by the heterogeneity of the contactor results in lower efficiency of the absorption which leads to an incorrect interpretation of overall absorption data. Schlünder [20] developed a mathematical model to estimate these effects in fixed beds, fluidised beds and bubble trays.

In membrane modules maldistribution can occur on both sides of the membrane; (1) the effect of the thickness of the membrane wall which effects the actual pore diameter in the lumen, and (2) local variations in the arrangement (pitch) of the membrane fibres resulting in preferential flow paths owing to different hydrodynamical resistances. The estimation of the effect of the latter phenomenon on maldistribution is very complicated and requires the availability of three-dimensional hydrodynamical one-phase flow models in combination with a mass transfer model. The estimation of the first effect on the performance of the membrane module will be discussed in this study.

The fibres can introduce a similar heterogeneity because they do not have exactly the same diameter. Moreover, the channels around the fibres do not have the same dimensions because the fibres are usually not installed regularly in the modules. With the same pressure difference between in- and outlet of the fibres or the channels, unequal flow rates through the fibres or the channels are obtained. This results in different degrees of saturation of the liquid at the outlet of the fibres. The flows of the individual fibres combine to give a mean degree of saturation. Mass transfer coefficients calculated from this degree of saturation may deviate substantially from the mass transfer coefficient obtained from the degree of saturation in a bundle of fibres having exactly the same diameter.

To show this phenomenon, the absorption in modules with fibres which have a certain diameter distribution, is mathematically analyses. Three distributions are considered. The first assumes a normal probability function for the fibre diameters:

$$f(d)=\frac{1}{\sigma\sqrt{2\pi}}\exp\left[-\frac{1}{2}\left(\frac{d-\bar{d}}{\sigma}\right)^2\right] \tag{5}$$

The second distribution assumed an equal probability for each diameter in the range of variation, $f(d)=$constant. In the third distribution only two fibres are considered with diameters equal to the boundary values for the first and second distribution. It must be noted, that this case is not encountered for the fibre modules available, it is only used as an illustrative example.

The degree of saturation in a fibre with a fully developed velocity profile is calculated with eqn. (6).

$$\frac{C(d)}{C_w}=1-\exp\left(-\frac{kA}{Q_v}\right)=1-\exp\left(-\frac{4kZ}{vd}\right) \tag{6}$$

The mass transfer coefficient k can be calculated from a generalised numerical solution of the Graetz–Lévèque equation. Curve fitting yields eqn. (7) which is also valid in the range of Gz numbers not covered by eqns. (4a) and (4b).

$$Sh=\frac{kd}{D}=\sqrt[3]{3.67^3+1.62^3Gz} \tag{7}$$

The velocity in the fibre is calculated from the Hagen–Poiseuille equation.

$$v=\frac{\Delta P d^2}{32\eta Z} \tag{8}$$

The contribution of each fibre to the degree of saturation in the outlet flow of the module is proportional to the volumetric flow rate and the degree of saturation per fibre. The degree of saturation in the combined outlet flow of the fibres follows from eqn. (9).

$$\frac{\bar{C}}{C_w}=\frac{\int_{\bar{d}-\Delta}^{\bar{d}+\Delta} d^4\frac{C(d)}{C_w}f(d)\partial d}{\int_{\bar{d}-\Delta}^{\bar{d}+\Delta} d^4 f(d)\partial d} \qquad (9)$$

The means mass transfer coefficient for the module can be calculated from this degree of saturation by eqn. (10).

$$\bar{k}_{distr}=-\frac{Q_v}{A}\ln\left((1-\frac{\bar{C}}{C_w}\right) \qquad (10)$$

Calculations were carried out in which the mean fibre diameter was taken equal to the diameter of one of the fibre types used in the experiments, 2.2×10^{-3} m. Unfortunately, no information was available on the distribution in pore diameter and wall thickness of the membrane material used in the present study. Therefore the range of diameter variation, Δ, was taken to be $\pm2\times10^{-4}$ m. In the normal probability distribution the standard deviation was taken such that on either side of the minimum and maximum diameter 5% of the distribution was neglected. The other parameters in these calculations were taken for the case of absorption of a gas in a liquid (diffusion coefficient $=10^{-9}$ m^2/sec and dynamic viscosity $=10^{-3}$ Pa-sec).

The ratio of the mass transfer coefficient from eqn. (10) and the mass transfer coefficient calculated for the mean fibre diameter is presented in Figs. 3(a), (b) and (c) as a function of fibre length for different mean liquid velocities and the diameter distributions used. These figures show a decrease of the ratio of the mass transfer coefficients with fibre length.

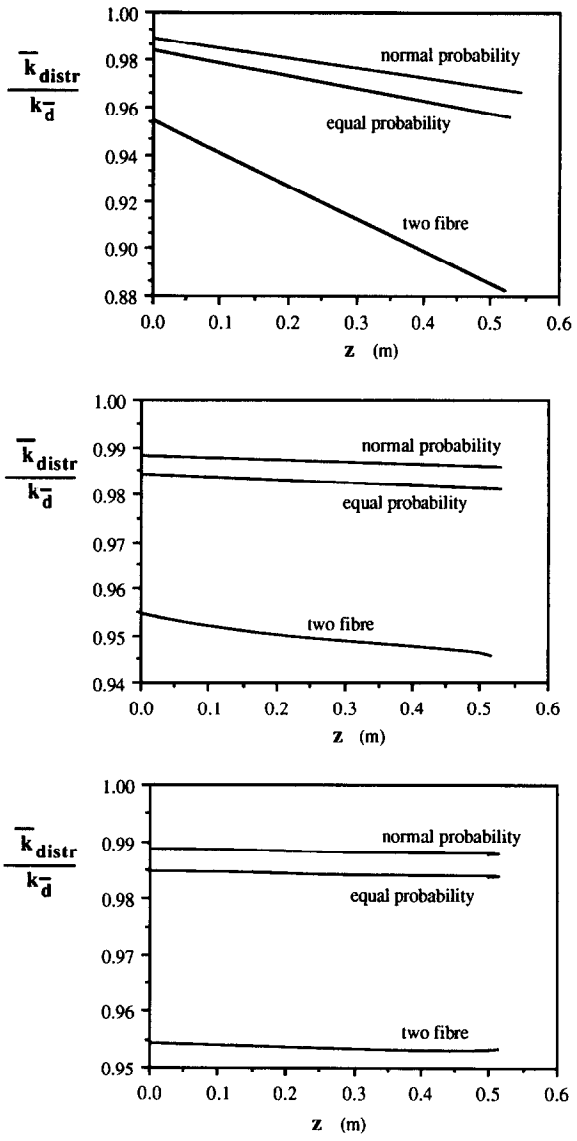

Fig. 3. Ratio of mass transfer coefficients in a bundle of fibres with different distributions of fibre diameters and a fibre with the mean diameter versus fibre length, mean liquid velocity (a) 10^{-3} m/sec, (b) 10^{-2} m/sec, (c) 10^{-1} m/sec.

This is caused by the fact that in longer fibres a larger degree of saturation is reached. Due to the logarithm in eqn. (10), small variations in the degree of saturation have a larger effect on the mass transfer coefficient if the degree of

saturation is closer to 1. The influence of the fibre distribution does not become negligible at very short fibre lengths, because still differences in saturation are present.

In each of the Figs. 3 the difference between the three kinds of distribution can be observed. The ratio of mass transfer coefficients differs more from unity for those fibre bundles that have more fibres with larger deviations of the mean diameter. Therefore the mass transfer coefficient of the two fibre distribution function shows the largest deviation from the mass transfer coefficient calculated for the mean diameter. In the normal probability distribution the smallest amount of fibres with largely deviating diameters are present.

The influence of the mean velocity on the ratio of mass transfer coefficients becomes more pronounced at lower velocities. Like with the influence of the fibre length, the degree of saturation becomes larger with lower velocities which has a larger effect on the ratio of mass transfer coefficients through the logarithm in eqn. (10).

If the unreal two fibre distribution is neglected, the maximum deviation calculated is about 5% for the lowest mean liquid velocity. This allows the use of the mean fibre diameter for the interpretation of the absorption experiments carried out in the present work.

With liquid flowing around the fibres this theoretical approach can also be applied. Differences in channel width of a factor 2 or higher are surely in the modules. However, it must be realised that the liquid-flows through the different channels around the fibres may be mixed partially while they pass through the module. This again influences the overall mass transfer.

Interpretation of absorption data in terms of mass transfer coefficients with mean or hydraulic diameters must be carried out carefully as the problem of unequal flow distribution can hardly be avoided.

5. Experiments

5.1. Hollow fibres and modules

Both modules and single fibres were studied in the experiments for which 3 different microporous fibres and one type of ultrafiltration fibre were used. The specifications of the fibres and the modules are given in Tables 1 and 2, respectively. Module A was constructed in our laboratory while module B was purchased from Akzo/Enka. To obtain a regular fibre packing in module A, two teflon discs were regularly perforated with holes just large enough to allow the fibres to pass through. Next the fibre bundle was aligned and potted in an open glass tube. The in- and outlet for the inside of the fibres were fitted at the ends of the glass tube. The module is shown in Fig. 4.

The experimental setup is shown in Fig. 5. The viscous liquids used are water/glycerol mixtures in which CO_2 is absorbed. The viscosity range covered, varied from 1 upto 68×10^{-3} Pa-sec at 25°C. The liquid is circulated from a stirred tank through the module back to the tank by a centrifugal pump or a tubing pump. The larger centrifugal pump was used when modules and the single fibre type III were used, the small tubing pump was applied when type, I, II and IV single fibres were used. In the stirred tank the absorbed CO_2 is desorbed by a nitrogen stream. The CO_2 concentration at the inlet of the module was determined by titration. This value was found to be negligible in relation to the degree of saturation reached during the absorption in the fibres. The gases were supplied from gas bottles. CO_2 is prewetted by a gas bubbler filled with the absorption liquid and then passed through the module.

The mass transfer coefficient is calculated according to eqn. (10). In the case of absorption with the single fibres the dimensionless liquid phase concentration in eqn. (10) was

TABLE 1

Membrane specifications

Code	Material	d_{in} (10^{-3} m)	d_{out} (10^{-3} m)	Surface porosity (-)	Pore diam. (m)
I	polypropylene	0.6	1.0	0.7	1×10^{-7}
II	polypropylene	2.2	2.6	0.7	1×10^{-7}
III	polypropylene	5.0	8.6	0.7	1×10^{-7}
IV	polysulfon	1.1	1.8	<0.03	$\sim5\times10^{-9}$

TABLE 2

Module specifications

Code	Fibre type	d_{module} (10^{-2} m)	Length (m)	Nr. of fibres	$a_{L\,in}$ (m^{-1})	$a_{L\,out}$ (m^{-1})	x_{fibres} (-)
A	I	4.0	0.35	38	209	247	0.16
B	II	1.4	0.30	85	817	1362	0.43

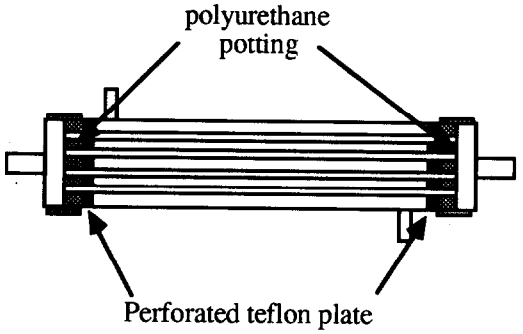

Fig. 4. Construction of a regularly spaced fibre module.

measured from pressure decrease in a confined gas volume around the fibre.

$$\frac{C_z}{C_w}=\frac{\mathrm{d}\ln\left(\frac{P}{P_o}\right)}{\mathrm{d}t}\frac{V_g}{mQ_v} \qquad (11)$$

In the case of absorption with the modules the dimensionless liquid phase concentration in eqn. (10) was measured from the volume of CO_2 absorbed at constant pressure indicated by a soap film meter.

$$\frac{C_z}{C_w}=\frac{\phi_{abs}}{mQ_v} \qquad (12)$$

The determination of solubility and diffusivity parameters of CO_2 in the glycerol/water mixtures is reported in Appendix B.

5.2. *Bubble column*

To compare the absorption capacity of a hollow fibre module with that of a bubble column, absorption experiments in a small scale bubble column were carried out in a similar setup like the one in Fig. 5. The column itself consisted of a glass pipe of 4×10^{-2} m inner diameter with a liquid hold-up of about 2×10^{-4} m^3. The gas was supplied to the column through a porous gas filter. The mass transfer was measured by the absorption of oxygen in the same liquids as those applied in the hollow fibre modules. The oxygen concentration in the liquid was measured with electrodes in the in- and outlet of the column. The signal of these electrodes is proportional to the oxygen content in the liquid (Halpert and Foley [21]). With the assump-

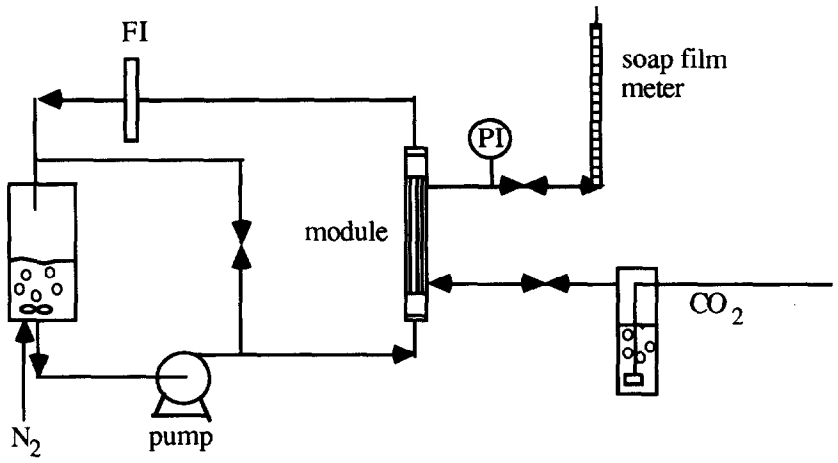

Fig. 5. Experimental setup.

tion of an ideally stirred liquid phase, $k_L a$ was calculated from eqn. (13).

$$k_L a = \frac{Q_v}{V_d(1-\epsilon_g)} \frac{(C_{out}-C_{in})}{(C_{sat}-C_{out})} \quad (13)$$

The depletion of the gas phase was negligible. Therefore an assumption on the behaviour of the gas phase: plug flow, ideally mixed or a situation in between of these limits was not needed for the interpretation of the experimental results.

6. Results

6.1. Hollow fibres and modules

During the absorption experiments with both the single fibres and the modules, the gas and liquid flow were always kept separate by the membrane. Never any stagnant bubble formation was observed in the liquids, which supports the applicability of this type of contactor for absorption. The hydrophobic material of the membranes prevents wetting of the membranes even at the higher liquid pressures needed to let the viscous liquids pass through the modules.

Exchanging area

In order to determine which area should be taken for the interpretation of absorption data to obtain mass transfer coefficients, absorption experiments of CO_2 in water with two single fibres with porosities of 70% and 3% (type I and IV respectively) were carried out. The mass transfer coefficients were calculated by taking the total membrane surface as exchanging area. The data are presented in Fig. 6 as *Sh* versus *Gz* number. The results obtained with both membranes correspond to the line predicted by theory, which is also drawn in Fig. 6 (eqns. 4).

Because pure gas is used in the present study, mass transfer is only determined by the resistance in the liquid phase. This situation is mathematically analysed by Wakeham and Mason [16]. In the liquid present in the fibres the CO_2 molecules diffuse according to the concentration gradient, which is present axial, tangential and radial in the liquid. Along the membrane wall (axial and tangential) saturation of the liquid is instantaneous compared to saturation in the radial direction, because the distance between two pores is much smaller than the distance between the fibre wall and the center of the tube. In Table 3 these data, derived with a triangular pitch of pores, are

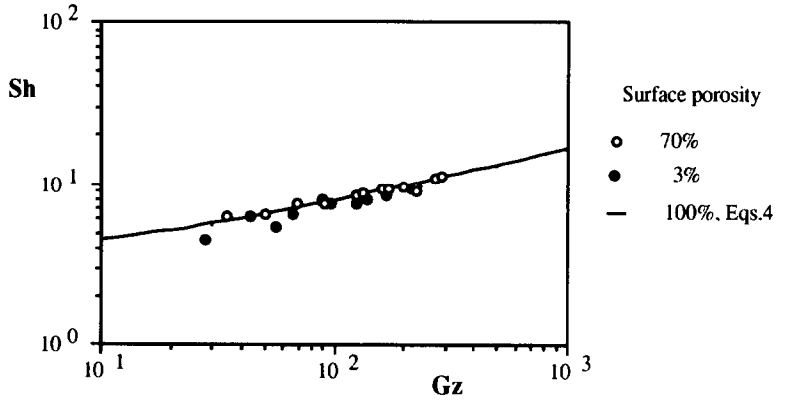

Fig. 6. Absorption data of CO_2 in water with two fibres with different surface porosities compared to the theoretical solutions, eqns. (4).

TABLE 3

Pore and porosity related data of two types of membranes

Membrane	Pore diameter (m)	Surface porosity (%)	Pore surface density (m^{-2})	Distance between two pores (m)
Polypropylene	1×10^{-7}	70	8.9×10^{13}	1.38×10^{-8}
Polysulfone	5×10^{-9}	3	1.5×10^{15}	2.25×10^{-8}

given together with the number of pores per area at the interface. Thus a very small liquid layer adjacent to the fibre wall can be considered as completely homogeneously saturated. From this layer the diffusion process into the flowing liquid takes place. In the further interpretation of absorption data the total membrane area will be used as the interfacial area through which the transport takes place. Keller and Stein [22], Malone and Anderson [23] and Lopez et al. [24] have considered analogous phenomenon.

Single fibres

In the absorption experiments with the different viscous liquids mass transfer coefficients were calculated according to eqn. (6) and translated into the dimensionless *Sh* and *Gz* numbers with the physical constants mentioned in Appendix B. The data calculated from the experiments are shown in Figs. 7(a), (b) and (c) for fibres I, II and III respectively. They are well described with eqn. (5a).

Modules with liquid through the fibres

In section 4 it was deduced that if only a minor spread of the diameter of the fibres in a bundle is present, no difference can be observed between the absorption in liquid flowing through the bundle or a single fibre of the mean diameter. The absorption data measured with modules of type I and II fibres are shown in Fig. 8. Like with the single fibres the experimental data are in close agreement with the theoretically derived solution (eqns. 4). It can be concluded that the difference in fibre diameters is negligibly small.

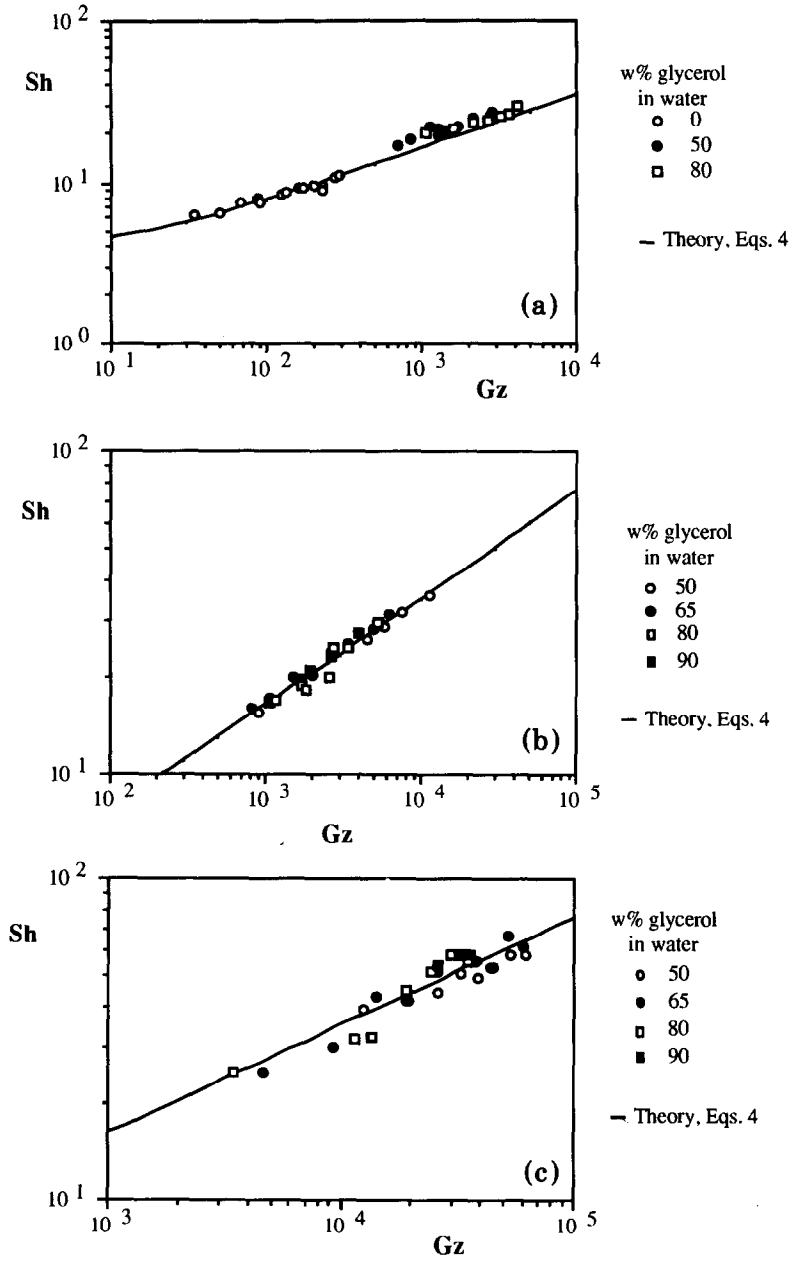

Fig. 7. Absorption data measured with a fibre of type I (Table 1) in different glycerol/water mixtures with a fibre of type (Table 1), (a) type I, (b) type II, (c) type III.

Modules with liquid around the fibres

The results of the experiments are presented in Figs. 9(a) and (b). In these figures also the relation derived by Miyatake and Iwashita [19] is plotted, modified for mass transfer outside the fibres in a bundle (Appendix A). The absorption in module A (Fig. 9a) with regularly placed fibres in a triangular pitch agrees well

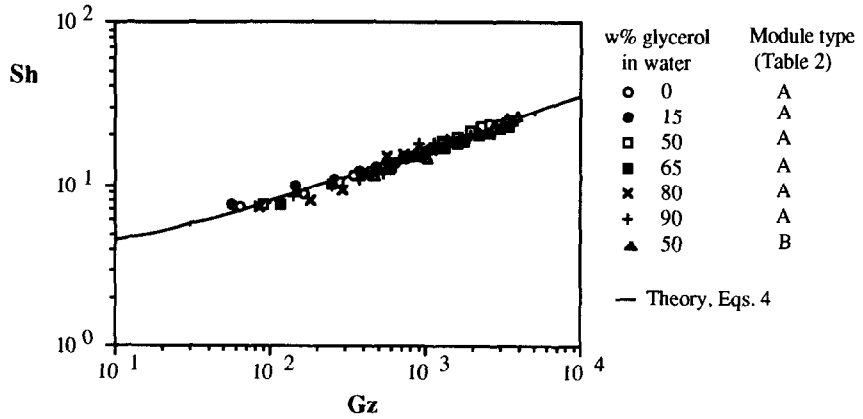

Fig. 8. Absorption data measured in two hollow fibre modules with different glycerol/water mixtures flowing *through* the fibres.

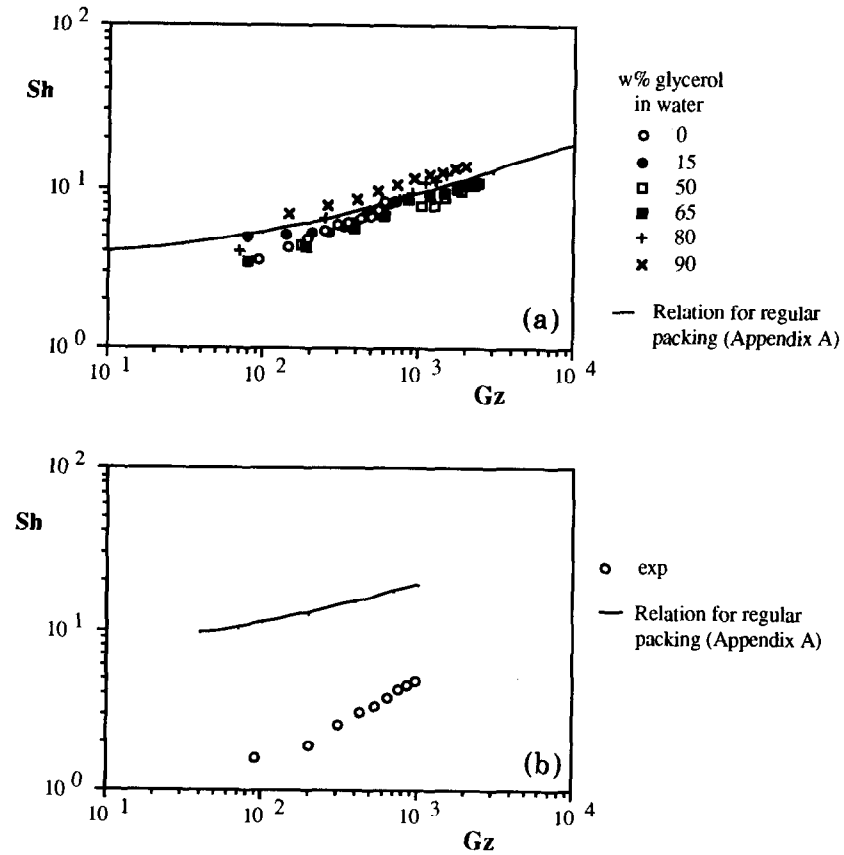

Fig. 9. (a) Absorption data measured in a *regularly* packed hollow fibre module with different glycerol/water mixtures flowing around the fibres. (b) Absorption data measured in an *irregular* packed hollow fibre module with a 50 wt.% glycerol/water mixture flowing around the fibres.

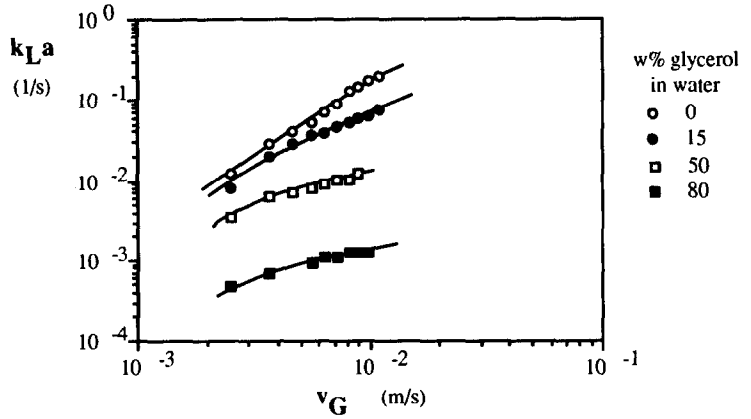

Fig. 10. Oxygen absorption measured in a bubble column with different glycerol water mixtures as a function of gas velocity.

with the theoretical solution of Miyatake and Iwashita. Small deviations must be attributed to in- and outlet effects and the influence of the wall of the module which are not incorporated in the theoretical equation.

The results obtained with module B (Fig. 9b) show a large difference with the solution of Miyatake and Iwashita. It can be concluded that the irregular packing of the fibres does not allow the use of the approach of Miyatake and Iwashita. The effects of the liquid distribution (section 4) must be considered to explain the absorption behaviour of modules with irregular packing of fibres.

6.2. *Bubble column*

Experimental k_La values obtained with absorption in the bubble column, are plotted in Fig. 10. The gas phase velocity could not be increased above 1.5×10^{-2} m/sec because foam formation occurred in the water/glycerol mixtures.

Mass transfer is positively influenced by the gas velocity but this effect is less pronounced in the more viscous liquids. Similar effects were measured by Buchholz et al. [25] and Voigt et al. [26], who also studied oxygen absorption in glycerol/water mixtures in bubble columns.

Mass transfer is also strongly dependent of viscosity. At the lowest gas phase velocity k_La differs a factor of 30 for the absorption in water and the 80% glycerol mixture, while at the highest velocities this factor is about 125.

If it is assumed that the diffusion coefficient of oxygen shows a similar decrease with the increase of the glycerol content as the diffusion coefficient of carbon dioxide in these liquids, the diffusion coefficient lowers a factor 10 between water and the 80 wt.% mixture. Calderbank et al. [27] correlated k_L with the square root of the diffusion coefficient, which means a decrease of k_L by a factor of about 3 between water and the 80% glycerol mixture. Thus not only the lower diffusion coefficient is responsible for the large decrease of k_La with increasing viscosity, but also the smaller interfacial area.

7. Discussion, bubble column versus membrane module

To compare the performance of the hollow fibre membrane module with the bubble column, absorption processes under similar conditions in these contactors must be studied. In the present work the degree of conversion that can be realized in the contactors was used as a

TABLE 4

Comparison of hollow fibre membrane module (hfmm) with bubble column (bc)

Liquid composition (wt.% glycerol)	Residence time (sec)	Liquid velocity (10^{-3} m/sec)	k_La		Degree of saturation	
			bc_{exp} (sec^{-1})	$hfmm_{calc}$ (sec^{-1})	bc_{exp} (-)	$hfmm_{calc}$ (-)
0	26	11.5	2.0×10^{-1}	2.3×10^{-2}	0.84	0.87
15	31	9.7	8.0×10^{-2}	2.0×10^{-2}	0.70	0.87
50	36	8.3	1.5×10^{-2}	6.5×10^{-3}	0.30	0.54
80	180	1.7	1.2×10^{-3}	2.0×10^{-3}	0.20	0.70

tool for comparison. No allowance has been made for additional aspects, e.g. pressure drop and the cost of investments. From the experimental results it is concluded that mass transfer in liquid flow through the fibres is described well with eqns. (4). In this section these relations are used to predict the absorption in a hollow fibre membrane module which can be compared to data for the bubble column used in the experiments. Therefore a membrane module with fibres of type I (Table 1) is assumed with the same liquid hold-up and liquid height as the bubble column used in the experiments. Such a module has a specific interfacial area of 2000 m^2/m^3 with a fibre length of 1.8×10^{-1} m.

From these data and eqns. (4) and (6), the mass transfer coefficient, k_La and the degree of saturation of oxygen in the water/glycerol mixtures can be calculated for the hollow fibre module. These results are compared with the experimental data of the bubble column in Table 4. It is assumed that the diffusion coefficient of oxygen shows a similar decrease with the increase of the glycerol content as the diffusion coefficient of carbon dioxide.

When viscosity increase, k_La decreases for both types of absorbers. However, while the interfacial area of the bubble column is also lowered by viscosity (section 6.2), in the fibre module this is not the case. Therefore, k_La of the module gets larger than k_La of the column.

Although in Table 4 only the k_La value for the most viscous glycerol/water mixture is higher for the hollow fibre membrane, the saturation which is obtained in both absorbers is always higher with the hollow fibre module. This effect is caused by the difference in the gas/liquid mixing in the absorbers. While the bubble column can be considered as a stirred tank, the contacting in the fibre module is better described with plug flow.

8. Conclusions

In the present study the applicability of hollow fibre membrane modules in gas/liquid contacting processes was investigated. These modules offer the possibility of an increased absorption capacity by applying small fibres in the modules which creates high interfacial areas. On the other hand, due to the small fibres and the narrow channels around the fibres, the phases on either side of the membrane are bound to flow laminarly, which may reduce the absorption capacity again.

In an absorption process carried out with a microporous membrane module no special attention has to be paid to the separation of gas and liquid phase. In the present work absorption in viscous liquids was studied, because in this field the gas/liquid contact in the membrane module looks very attractive. Since gas and liquid flow are separated by the membrane

no stagnant gas bubbles were formed in the liquid nor was any foam formation observed. These two phenomena are known from industrial practice while they were also observed in the application of the more viscous liquids in a lab scale bubble column.

From the absorption experiments carried out in the membrane modules it was concluded that although the gas is only in contact with the liquid at the pore mouths, which cover the area only partially, the total membrane area has to be used as the exchanging area for the determination of the mass transfer coefficient. Diffusion takes place effectively from the liquid layer adjacent to the fibre wall which is homogeneously saturated, because the distances between the pores are extremely small compared to the distance for diffusion to the centre of the fibre.

For predicting mass transfer in laminar flow through a single fibre, the Graetz–Lévèque equation can be used which was originally developed for heat transfer. In a module, however, due to small variations in fibre diameters, differences in saturation per fibre can occur. With the aid of a mathematical model it was demonstrated, that these differences were negligible compared to the experimental accuracy and thus the Graetz–Lévèque equation can also be used in the case of a bundle of fibres in a module. Mass transfer in a laminarly flowing liquid around regularly packed fibres can be estimated satisfactory with the results of the numerical solution for the similar heat transfer problem obtained by Miyatake and Iwashita [19]. Normally produced hollow fibre modules have irregular fibre packings and therefore a wide variation of the dimensions of the channels occurs leading to substantial differences in flow rates. Therefore the method of Miyatake and Iwashita [19] cannot be used and it is very difficult to predict mass transfer in liquid flowing around irregularly packed fibres.

If the absorption capacity of the membrane module and the bubble column are compared in terms of $k_L a$, the module only shows a better performance for more viscous liquids. This is caused by the fact that the mass transfer coefficient and the interfacial area in the bubble column are reduced while in the membrane module only the mass transfer coefficient is affected by an increasing viscosity.

Absorption capacity can also be compared in terms of the degree of saturation that can be obtained in both absorbers. Because of the difference in the mixing pattern, ideal mixing for the bubble column and plug flow for the membrane module, a higher degree of saturation in the membrane module is reached in a case with an equal mean residence time for the liquid.

Acknowledgements

These investigations were supported by TNO the Netherlands organization for applied scientific research. We also acknowledge G. Schorfhaar for the construction of the experimental setup and E. Kippers for his part in the experimental work.

List of symbols

A	membrane area (m^2)
C	concentration (mol/m^3)
d	fibre diameter (m)
D	diffusion coefficient (m^2/sec)
Gz	Graetz number (–)
Gz'	idem, defined in Appendix
J	absorption flux (mol/m^2-sec)
k	mass transfer coefficient (m/sec)
m	distribution coefficient (–)
Nu	Nusselt number
P	pressure (N/m^2)
Q_v	volumetric flow rate (m^3/sec)
r	radial coordinate (m)
R	fibre radius (m)
Re	Reynolds number (–)
s	half pitch between fibres (–)

S	wetted circumference (m)
Sc	Schmidt number (-)
Sh	Sherwood number (-)
t	time coordinate (sec)
v	velocity (m/sec)
V	volume (m^3)
z	axial coordinate (m)
Z	fibre length (m)
α	diameter ratio (-)
Φ	Absorption flow (m^3/sec)
ϵ	hold up (-)
μ	dynamic viscosity (Pa-sec)
ρ	density (kg/m^3)
σ	standard deviation (-)
Σ	pitch to diameter ratio (-)
Φ	$\Sigma-1$ (-)

Indices

abs	absorption
d	dispersion
distr	distributed
g	gas phase
in	inlet stream
L	liquid phase
m	mean value
out	outlet stream
r	radial
sat	saturated
th	theoretical
tot	total
v	volumetric
w	at the wall of the fibre

References

1 H. Kreulen, G.F. Versteeg, C.A. Smolders and W.P.M. van Swaaij, Determination of mass transfer rates in wetted and non-wetted microporous membranes, Chem. Eng. Sci., 1993 (in press).

2 A. Laurent and J.C. Charpentier, Aires interfaciales et coefficients de transfert de matière dans les divers types d'absorbeurs et de réacteurs gaz-liquide, Chem. Eng. J, 8 (1974) 85.

3 H. van Landeghem, Multiphase reactors: Mass transfer and modelling, Chem. Eng. Sci., 35 (1980) 1912.

4 S.L. Matson, J. Lopez and J.A. Quinn, Separation of gases with synthetic membranes, Chem. Eng. Sci., 38 (1983) 503.

5 L. Graetz, Uber die Wärmeleitungsfähigkeit von Flüssigkeiten, 1e Abhandlung, Annalen der Physik und Chemie, 18 (1883) 79.

6 L. Graetz, Uber die Wärmeleitungsfähigkeit von Flüssigkeiten, 2e Abhandlung, Annalen der Physik und Chemie, 25 (1885) 337.

7 J. Lévèque, Les lois de la transmission de chaleur par convection, Annls. Mines, Paris (Series 12) (1928) 201, 305, 381.

8 M. Jakob, 1949, Heat Transfer, Academic Press New York, NY, Vol. I.

9 E.N. Sieder and G.E. Tate, Heat transfer and pressure drop of liquids in tubes, Ind. Eng. Chem., 28 (1936) 1429.

10 W.H. Linton Jr. and T.K. Sherwood, Mass transfer from solid shapes to water in streamline and turbulent flow, Chem. Eng. Progr., 46 (1950) 258.

11 M.R. Goldman and L.R. Barret, Mass transfer with concentration dependent properties in streamline flow, Trans. Inst. Chem. Eng., 47 (1969) T29.

12 N.C. Kafes and C.W. Clump, Turbulent and laminar mass transfer in a tubular membrane, AIChE J., 19 (1973) 1247.

13 M.C. Yang and E.L. Cussler, Designing hollow fibre contactors, AIChE J., 32 (1986) 1910.

14 Q. Zhang and E.L. Cussler, Microporous hollow fibres for gas absorption. I. Mass transfer in the liquid, J. Membrane Sci., 23 (1985) 321.

15 H. Kreulen, 1993, Microporous membranes in gas separation using a liquid phase, Ph. D. Thesis, Twente University, Enschede, The Netherlands.

16 W.A. Wakeham and E.A. Mason, Diffusion through multiperforate laminae, Ind. Eng. Chem. Fundam., 18 (1979) 301.

17 C.S. Lin, E.B. Denton, H.S. Gaskill and G.L. Putnam, Diffusion-controlled electrode reactions, Ind. Eng. Chem., 43 (1951) 2136.

18 T. Mizushina, The electrochemical method in transport phenomena, in: T.F. Irvine and J.P. Hartnett (Eds.), Advances in Heat Transfer, Vol. 7, Academic Press, New York, NY, 1971.

19 O. Miyatake and H. Iwashita, Laminar-flow heat transfer to a fluid flowing axially between cylinders with a uniform surface temperature, Int. J. Heat Mass Transf., 33 (1990) 416.

20 E.U. Schlünder, On the mechanism of mass transfer in heterogeneous systems. In particular fixed beds, fluidised beds and on bubble trays, Chem. Eng. Sci., 32 (1977) 845.

21 G. Halpert and R.T. Foley, The detection of oxygen by gas phase polarography at low temperatures and low pressures, J. Electroanal. Chem., 6 (1963) 426.

22 K.H. Keller and T.R. Stein, A two-dimensional analysis of porous membrane transport, Math. Biosciences, 1 (1967) 421.
23 D.M. Malone and J.L. Anderson, Diffusional boundary-layer resistance for membranes with low porosity, AIChE J., 23 (1977) 177.
24 J.L. Lopez, S.L. Matson, J. Marchese and J.A. Quinn, Diffusion through composite membranes. A two-dimension analysis, J. Membrane Sci., 27 (1986) 301.
25 H. Buchholz, R. Buchholz, H. Niebeschütz and K. Schügerl, Absorption of oxygen in highly viscous Newtonian and non-Newtonian fermentation model media in bubble column bioreactors, Eur. J. Appl. Microbiol. Biotechnol., 6 (1978) 115.
26 J. Voigt, V. Hecht and K. Schügerl, Absorption of oxygen in countercurrent multistage bubble columns. II, Aqueous solutions with high viscosity, Chem. Eng. Sci., 35 (1980) 1317.
27 P.H. Calderbank, D.S.L. Johnson and J. Loudon, Mechanisms and mass transfer of single bubbles in free rise through Newtonian and non-Newtonian liquids, Chem. Eng. Sci., 25 (1970) 235.
28 P.H. Calderbank, Mass transfer coefficients in gas–liquid contacting with and without mechanical agitation, Trans. Inst. Chem. Eng., 37 (1959) 173.
29 R.A.T.O. Nijsing, R.H. Hendriksz and H. Kramers, Absorption of CO_2 in jets and falling films of electrolyte solutions, with and without chemical reaction, Chem. Eng. Sci., 10 (1959) 88.
30 R.B. Bird, W.E. Stewart and E.N. Lightfoot, Transport Phenomena, Wiley & Sons, New York, NY, 1960.
31 G.F. Versteeg and W.P.M. Van Swaaij, Diffusivity and solubility of acid gases in aqueous amine solutions. J. Chem. Eng. Data, 33 (1988) 29.

Appendix A

Heat transfer correlations of Miyatake and Iwashita [19] modified for mass transfer

In this appendix the heat transfer correlations derived by Miyatake and Iwashita [19] are given, modified for mass transfer. Different equations were obtained for triangular and square arrangement of the cylinders and different ranges of the relative distance between the cylinders, Σ. The fibres in the regularly packed module used in the present study were arranged in a triangular array.

Triangular array, $1.0 \leqslant \Sigma \leqslant 1.1$:

$$Sh = 9.26(1 + 0.0179 Gz'^{1.46})^{1/4}$$

Square array, $1.0 \leqslant \Sigma \leqslant 1.2$:

$$Sh = 4.08(1 + 0.0349 Gz'^{1.46})^{1/4}$$

Triangular array, $1.1 < \Sigma \leqslant 4.0$ and square array, $1.2 < \Sigma \leqslant 4.0$:

$$Sh = \left\{ f^2 + \left(\frac{3g}{2}\right)^2 Gz'^{2/3} \right\}^{1/2}$$

Triangular array:

$$f = \frac{8.92(1 + 2.28\Phi)}{1 + 6.86\Phi^{5/3}}$$

$$g = \frac{2.34(1 + 24\Phi)}{(1 + 36.5\Phi^{5/4})(2\sqrt{3}\Sigma^2 - \pi)^{1/3}}$$

Square array:

$$f = \frac{4.00(1 + 0.509\Phi)}{1 + 0.765\Phi^{5/3}}$$

$$g = \frac{1.69(1 + 9.1\Phi)}{(1 + 10.8\Phi^{5/4})(4\sigma^2 - \pi)^{1/3}}$$

$$\Phi = \Sigma - 1$$

Appendix B

Solubility and diffusivity of CO_2 in glycerol–water mixtures at 298 K

In deriving the Sherwood relations for mass transfer in hollow fibre modules which were operated at 25°C, the diffusion coefficient of CO_2 in the glycerol/water mixtures is needed. Values in mixtures with a glycerol content between 0 and 70% have been reported by Calderbank [28], who derived the data from experiments in a liquid-jet. In the present study diffusion coefficients for mixtures with higher glycerol

TABLE B-1

Physical data at 25 °C of glycerol/water mixtures

Liquid comp. (wt.% glyc/water)	m_{CO_2} (-)	μ (10^{-3} N-sec/m^2)	ρ (kg/m^3)
0/100	0.82	0.89	997
15/85	0.73	1.34	1034
50/50	0.47	6.46	1138
65/35	0.44	13.2	1169
80/20	0.35	36.2	1201
90/10	0.28	68.2	1217

TABLE B-2

Diffusion coefficients for CO_2 in glycerol/water mixtures at 25 °C

wt.% glycerol	μ (10^{-3} N-sec/m^2)	D (10^{-10} m^2/sec)	Reference
9.5	1.1	17.1	Calderbank [28]
19.3	1.5	13.4	Calderbank [28]
20	1.38	13.8	Present study
28.0	2.1	9.34	Calderbank [28]
45.0	4.0	6.05	Calderbank [28]
54.0	6.2	4.99	Calderbank [28]
60.4	9.2	3.88	Calderbank [28]
64.4	12.0	2.88	Calderbank [28]
67.6	15.4	2.32	Calderbank [28]
70.4	19.2	1.52	Calderbank [28]
78.7	31.5	1.33	Present study
83.7	57.9	1.07	Present study
87.5	91.0	0.65	Present study

contents are reported. These were determined in experiments with a laminar film reactor.

For the determination of diffusion coefficients from absorption experiments the laminar film reactor is widely used as a model reactor because the interfacial area and the hydrodynamics of the liquid phase are known, see e.g. Nijsing et al. [29] and Bird et al. [30]. From the experiments the product of solubility and the square root of the diffusion coefficient can be derived. Therefore the solubility must be measured separately in order to be able to calculate the diffusion coefficients. In the present study the solubility of CO_2 in glycerol/water mixtures was determined in a stirred cell as described by Versteeg and Van Swaaij [31].

The results of the solubility experiments are reported in Table B-1. The solubility is expressed as the distribution coefficient, the ratio of concentration in liquid and gas phase at equilibrium. Viscosity and density of the glycerol/water system are also reported in Table B-1. Viscosity was determined using Ubbelohde viscosimeters and density was measured in pycnometers. Both apparatus were submerged in a thermostatted water bath, which was operated at 25 °C. The mixtures used, were taken from the mass transfer experiments. For the

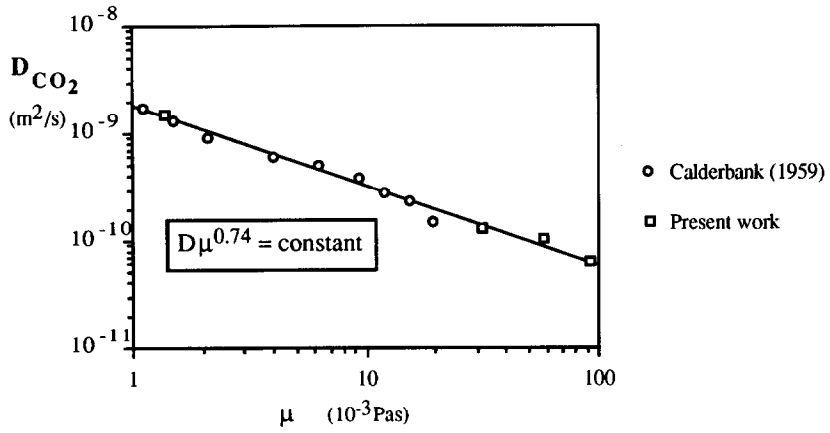

Fig. B-1. Diffusion coefficient of CO_2 as a function of viscosity in glycerol/water mixtures at 25°C.

experiments in the laminar film reactor fresh glycerol/water mixtures were prepared.

The diffusion coefficients determined in the present study are given in Table B-2 with the viscosity of the mixture. This table also includes the data determined by Calderbank [28]. Both sets of data are presented in Fig. B-1. A modified Stokes–Einstein correlation determined from the data of Calderbank also holds for the diffusion coefficient at higher viscosities ($D\eta^{\alpha}$=constant, with α=0.74).